Imminent phenomenology of a minimal gauge-mediated model

Emidio Gabrielli*
Departamento de Física Teórica, Universidad Autónoma de Madrid, Cantoblanco, 28049 Madrid, Spain

Uri Sarid†
Department of Physics, University of Notre Dame, Notre Dame, Indiana 46556
(Received 13 May 1998; published 13 October 1998)

We calculate the inclusive branching ratio for $B\to X_s\gamma$, the inclusive branching ratios and asymmetries for $B\to X_s\ell^+\ell^-$, and the anomalous magnetic moment $g_\mu-2$ of the muon, within a minimal gauge-mediated supersymmetry-breaking model which naturally generates a large ratio $\tan\beta$ of Higgs field vacuum expectation values. These predictions are highly correlated with each other, depending on only two fundamental parameters: the superpartner mass scale and the logarithm of a common messenger mass. The predictions for $B\to X_s\gamma$ decay and $g_\mu-2$ are in somewhat better agreement with current experiments than the standard model, but a much sharper comparison will soon be possible using new measurements now in progress or under analysis. Moreover we predict large deviations in $B\to X_s e^+e^-$ and $B\to X_s\mu^+\mu^-$ asymmetries, and somewhat smaller ones in $B\to X_s e^+e^-$ and $B\to X_s\tau^+\tau^-$ branching ratios, which will be detectable in hadronic colliders. [S0556-2821(98)00521-9]

PACS number(s): 12.60.Jv, 14.40.Nd, 14.60.Ef

I. INTRODUCTION

Arguably the least-understood aspects of supersymmetry (SUSY) as a physically acceptable theory are the mechanisms which break SUSY and which communicate that breaking to the observable sector. These mechanisms must generate soft-breaking mass terms which are small enough to protect the Higgs boson mass, large enough to have evaded all direct searches so far, and flavor symmetric enough to respect all current indirect bounds. In particular, flavor-changing neutral current (FCNC) processes impose strong constraints on any nonuniversal soft-breaking masses, due to gluino- and photino-mediated SUSY contributions [1]. Moreover CP-violating phases in the soft-breaking sector must be strongly suppressed to satisfy the constraints on electric dipole moments [1].

In supergravity-mediated scenarios with a flat Kähler metric [2] the SUSY breaking is communicated from the hidden sector to the observable one by gravitational interactions, leading to universality in the soft-breaking sector near the Planck scale. But even such a strong assumption about physics at extremely high scales may not be sufficient to prevent large flavor violations at observable scales. Indeed in grand-unified supersymmetric theories [3], the large top Yukawa couplings and radiative effects above the unification scale can generate unacceptably large FCNC and CP-violating processes. Moreover it is doubtful whether supergravity theories derived from superstrings would have flat Kähler metrics and flavor-independent supersymmetry-breaking terms [4].

Recently there has been a revival of interest in a class of models which can solve both the SUSY flavor and CP problems: theories of gauge-mediated SUSY breaking [5–9]. In these theories the SUSY-breaking sector is coupled to the observable [minimal supersymmetric standard model (MSSM)] sector via gauge interactions. Many models employ the standard-model (SM) gauge interactions to couple the MSSM to a messenger sector, which then couples more directly to the SUSY-breaking sector (much as in the gravitationally mediated picture the MSSM and the SUSY-breaking hidden sector communicated only via Planck-scale physics). The messenger sector may be far below the Planck scale, thus also lowering the SUSY-breaking scale, and the gauge interactions which generate observable SUSY-breaking masses are naturally flavor blind, thus preserving the approximate flavor symmetries of the SM. In the class of models studied in this work, the ultimate source of SUSY breaking is parametrized by a superfield $\hat{S}$ whose scalar and F components both acquire vacuum expectation values (VEVs) through an unspecified mechanism. Since this superfield is a SM gauge singlet with no direct couplings to the observable sector, the mechanism of SUSY breaking is largely isolated from, and therefore unconstrained by, the known properties of the SM. $\hat{S}$ does couple to a set of messenger fields, which do carry SM gauge quantum numbers. When their superpartners are split by the couplings to $\hat{S}$, they radiatively split the MSSM gauginos from the gauge bosons and the sfermions from the SM fermions, thus conveying SUSY breaking to the particles we observe.

The pattern of SUSY breaking in the MSSM produced by gauge mediation is thus exactly what is needed to solve the SUSY flavor and CP problems. Moreover the most minimal of these models are highly predictive, since most of the MSSM parameters beyond the SM depend on only the scale of the messenger masses and of the SUSY-breaking VEV (and the number of messenger fields). Unfortunately neither the superpotential μ term, which is the coupling between the up- and down-type Higgs superfields, nor the soft-breaking

*Electronic address: emidio.gabrielli@roma1.infn.it, egabriel@delta.ft.uam.es
†Electronic address: sarid@particle.phys.nd.edu

term $B\mu$, which couples the scalar Higgs fields, is generated by the usual gauge mediation mechanism: both couplings violate the Peccei-Quinn (PQ) symmetry of relative rotations between the Higgs doublets, which gauge interactions preserve. But for phenomenological reasons μ must be generated somehow, and indeed a few dynamical mechanisms have been proposed to break the PQ symmetry at the proper scale [10,9]. Possible solutions of this μ problem are an active area of research in this field.

We will regard the μ term as a free parameter, to be fixed phenomenologically by requiring that the electroweak vacuum be broken at the correct scale by radiative corrections. We will then assume, as in Ref. [11], that when the μ term is generated the corresponding $B\mu$ term is not (and also the soft-breaking Higgs boson masses are unaltered). Of course $B\mu$ will be induced radiatively, but since we assume that its boundary value at the messenger scale vanishes, we can predict its value at lower, observable scales [11]. The vanishing of $B\mu$ at the messenger scale offers several attractions:

(1) The two physical SUSY CP-violating phases $\arg(BM_{1/2}^*)$ and $\arg(AM_{1/2}^*)$, where $M_{1/2}$ is a gaugino mass and A is the scalar analogue of the Yukawa couplings in the superpotential, are zero [7], solving completely the SUSY CP problem.

(2) All soft-breaking terms and relative signs can be predicted essentially in terms of only two parameters, a common messenger mass and the SUSY-breaking scale.

(3) Since $B\mu$ at observable scales turns out to be small, $\tan\beta$, the ratio between the up- and down-type Higgs VEVs, is naturally predicted to be large, thus generating the observed large hierarchy between top and bottom quark masses without appealing to hierarchical Yukawa couplings.

Since a naturally large $\tan\beta$ is a signature of this model, we analyze a class of low-energy processes which are particularly sensitive to large $\tan\beta$. It is well known that in the MSSM the processes mediated by magnetic dipole transitions can be enhanced by $\tan\beta$. The corresponding SM amplitudes are chiral suppressed, while some of the SUSY contributions can receive a $\tan\beta$ enhancement, making the new contributions competitive with the standard ones. Within this class of processes, we consider in the framework of the minimal gauge mediated (MGM) model the radiative $b\to s\gamma$ and semileptonic $b\to sl^+l^-$ decays (with $l=e,\mu,\tau$) and the contribution to the anomalous magnetic moment of the muon $g_\mu-2$. For the $b\to s\ell^+\ell^-$ processes we analyze both the decay rate and the energy or forward-backward (FB) asymmetries.

In $b\to s\gamma$ and $g_\mu-2$ the corresponding amplitudes are proportional to the magnetic dipole transitions and so are directly enhanced by $\tan\beta$. The $b\to sl^+l^-$ amplitude receives contributions from both the local four-quark operators Q_9 and Q_{10}, which are not enhanced by $\tan\beta$ and in fact will be largely unaffected by the MGM, and from the same magnetic-dipole operator Q_7 responsible for the $b\to s\gamma$ decay. (Q_7 contributes to the $b\to s\ell^+\ell^-$ amplitude through the exchange diagram between Q_7 and the electromagnetic lepton current.) Therefore the sensitivity of $b\to s\ell^+\ell^-$ to $\tan\beta$ is correlated with that of $b\to s\gamma$ through their common dependence on a single Wilson coefficient.

A number of studies for $b\to s\gamma$ [12–15], $b\to s\ell^+\ell^-$ [12,16–19], and $g_\mu-2$ [20–23] have already been carried out for MSSM models similar to the one we consider. But our analysis for the MGM model is unique in its predictivity: there are essentially only two parameters, and they determine a tight correlation between these processes. (Moreover in our analysis we include the complete next-to-leading order accuracy in the strong coupling for the SM contribution to $b\to s\gamma$ [24] and $b\to sl^+l^-$ [25,26].) Present data *mildly* favor our predictions over those of the SM. Measuring the correlated deviations in these processes from SM predictions will either favor this model over the standard one and measure its parameters, or strongly constrain the model by forcing it to agree closely with the SM, or disfavor both this model and the standard one.

The paper is organized as follows. In the next section we define the model and give the analytical results for the mass spectrum of squarks, sleptons, Higgs bosons, and gauginos at the physical scale. We state these results for the mildly more general model than the minimal one, allowing for $N>1$ messenger families. All these quantities are expressed as a function of the SUSY-breaking scale Λ (or equivalently the W-ino mass) and the common messenger mass. Also in this section we give the numerical predictions for the magnitude of the μ parameter (for various values of N, messenger scale and top quark mass) and a detailed discussion about the predictions of its sign. In Secs. III–V we analyze the contribution of the MGM model to the $b\to s\gamma$, $b\to s\ell^+\ell^-$ decay rates and asymmetries, and $g_\mu-2$, respectively. We give model-independent parametrizations for the total rates and asymmetries and analytical expressions for the MGM contributions to the corresponding amplitudes in a suitable approximation. In Sec. VI we present and analyze the numerical predictions for the $b\to s\gamma$ and $b\to s\ell^+\ell^-$ decay rates and asymmetries versus the $g_\mu-2$ ones, as a function of the SUSY-breaking scale and the common messenger mass in both $N=1$ and $N=2$ scenarios. The final section contains our conclusions and outlook.

II. MINIMAL GAUGE MEDIATED MODEL

In gauge-mediated supersymmetry breaking (GMSB) models supersymmetry is broken at some scale above the electroweak scale and then the breaking is communicated to the MSSM particles by the usual SM gauge interactions [5–9]. In the minimal realization of this idea, a pair of SU(2) doublet chiral superfields Φ_2, $\overline{\Phi}_2$ and a pair of SU(3) triplet chiral superfields Φ_3, $\overline{\Phi}_3$, called messenger fields, couple to a singlet chiral superfield $\hat{S}$ with Yukawa couplings $\lambda_{2,3}$. The messenger fields get their supersymmetric mass through the VEV $\langle S\rangle$ of the scalar component of the $\hat{S}$ superfield. But the F component of $\hat{S}$ also has a nonvanishing VEV $\langle F\rangle$ which parametrizes the breaking of supersymmetry. The breaking is manifest in the consequent mass splitting between the fermionic and scalar component of the messenger fields Φ_i: the fermions of Φ_i acquire masses $M_{M_i}=\lambda_i\langle S\rangle$

while their scalar partners get squared masses $m_i^2 = |\lambda_i \langle S \rangle|^2 \pm |\lambda_i \langle F \rangle|$.

In this minimal gauge-mediation model, the messenger fields couple at tree level only with the gauge sector of the MSSM and not with its matter fields. Thus SUSY breaking is transmitted to the MSSM only by the ordinary gauge interactions. At one loop, gaugino masses are generated by finite self-energy diagrams, with the fermionic and scalar components of the messenger fields running in the loop. In the following we will allow the possibility of $N \geqslant 1$ messenger families (pairs of doublets and triplets), but only a single source $\hat{S}$ of SUSY breaking. We will also assume that the messengers are approximately degenerate; our results are not very sensitive to this splitting as long as the messengers are not very split and not very close to their lower bound (see below). We denote quantities evaluated at the messenger scale by an overbar. Then the gaugino mass spectrum $\overline{M}_i$ is given by

$$\overline{M}_i = N \overline{\frac{\alpha_i}{4\pi} \Lambda g(x_i)} \equiv \hat{M}_i g(x_i), \tag{1}$$

where $\Lambda \equiv \langle F_S \rangle / \langle S \rangle$ and $x_i = \Lambda / M_{M_i}$. The function $g(x)$ contains the result of the one-loop integration [8]. Its argument must satisfy $x_i < 1$ to ensure that the messenger scalars have a positive mass squared. We will not be concerned with M_{M_i} just above but very close to the minimal value Λ, so x_i will never approach unity, in which case $g(x_i) \simeq 1$ and $\overline{M}_i \simeq \hat{M}_i$ will be very good approximations.

At two-loop order in the messenger fields, or more plainly at one-loop order in the gaugino masses, squark, slepton and Higgs SUSY-breaking *squared* masses are generated by self-energy diagrams with a gaugino mass insertion. Thus the sfermion masses (rather than their squares) are the same order as the gaugino masses. Once again we are concerned with x_i well below unity, in which case the results of the sfermion mass calculation can be expressed as [11]

$$\overline{m}_\alpha^2 \simeq \frac{1}{N} \left(2C_3 \hat{M}_3^2 + 2C_2 \hat{M}_2^2 + \frac{6}{5} Y^2 \hat{M}_1^2 \right), \tag{2}$$

where the coefficients C_i depend on the gauge quantum numbers of the scalar multiplets and Y is the weak hypercharge. Explicitly, these equations read

$$\overline{m}_{\tilde{Q}}^2 = \mathbf{1} \frac{1}{N} \left(\frac{8}{3} \hat{M}_3^2 + \frac{3}{2} \hat{M}_2^2 + \frac{1}{30} \hat{M}_1^2 \right), \tag{3}$$

$$\overline{m}_{\tilde{u}}^2 = \mathbf{1} \frac{1}{N} \left(\frac{8}{3} \hat{M}_3^2 + \frac{8}{15} \hat{M}_1^2 \right), \tag{4}$$

$$\overline{m}_{\tilde{d}}^2 = \mathbf{1} \frac{1}{N} \left(\frac{8}{3} \hat{M}_3^2 + \frac{2}{15} \hat{M}_1^2 \right), \tag{5}$$

$$\overline{m}_{\tilde{L}}^2 = \mathbf{1} \frac{1}{N} \left(\frac{3}{2} \hat{M}_2^2 + \frac{3}{10} \hat{M}_1^2 \right), \tag{6}$$

$$\overline{m}_{\tilde{l}}^2 = \mathbf{1} \frac{1}{N} \left(\frac{6}{5} \hat{M}_1^2 \right), \tag{7}$$

$$\overline{m}_{H_U}^2 = \overline{m}_{H_D}^2 = \frac{1}{N} \left(\frac{3}{2} \hat{M}_2^2 + \frac{3}{10} \hat{M}_1^2 \right) \tag{8}$$

for the squared masses of the squark doublet, the up- and down-type squark singlets, the slepton doublet, the charged slepton singlet, and the up- and down-type Higgs doublets. We have also explicitly inserted the unit matrix **1** in flavor space: the gauge interactions which generate these masses are flavor blind.

Another consequence of the pure gauge mediation in the MGM is that the SUSY-breaking A terms which couple the squarks (or sleptons) to the Higgs doublets are not induced at the same order as the gaugino or sfermion masses, since they break the chiral (flavor) symmetries while the gauge interactions do not. A terms are induced at higher order via gaugino masses, so both A and $\hat{M}$ arise through the same source Λ, and hence the relative CP-violating phase between them $\arg(A_i^* M_3)$ vanishes naturally.

The μ parameter, which couples the up- and down-type Higgs doublet superfields in the superpotential, is not generated within the GMSB paradigm, since it breaks the Peccei-Quinn symmetry while the gauge interactions do not. To have a (phenomenologically mandated) nonvanishing μ term, the MGM model must be extended. We will *assume* that such an extension does not have any impact on the mass parameters beyond the μ term (but see Ref. [10] for counterexamples). Thus effectively μ is an arbitrary additional parameter of the model, as was assumed in most of the previous literature. But in fact its value can be predicted by the phenomenological requirement that the electroweak vacuum should spontaneously break to yield the proper Higgs boson VEV.

The SUSY-breaking analogue of the μ term, the $B\mu$ term coupling the Higgs doublets in the scalar potential, is also not generated by the pure MGM. We will *assume*, as we did above, that whatever mechanism generates μ does *not* generate $B\mu$, and this is the major assumption of this work. While this is by no means a generic aspect of GMSB models (see Ref. [10] for a critical analysis of this issue), it is theoretically conceivable since $B\mu$ would break an R symmetry which μ would not (see Ref. [7] for an example and Ref. [11] for further discussion). It is also phenomenologically appealing, since (as for the A terms) B is generated radiatively through gaugino masses, and hence the CP-violating relative phase $\arg(B^* M_3)$ once again vanishes naturally. Thus the SUSY CP problem is completely absent in this model. To reiterate: in the following we will always assume the boundary condition $\overline{B} \simeq 0$.

Notice that the only source of phases (apart from topological vacuum angles) is the SM CP-violating phase in the quark Yukawa couplings. In particular, no physical relative signs are arbitrary parameters; thus the relative sign between μ, the Higgs VEVs and the gaugino masses (which is often just called the sign of μ) is a *prediction* of this model, which we calculate below.

Since the messenger scale is considerably higher than the electroweak scale, we use the above MSSM parameters as boundary conditions to the renormalization group (RG) evolution equations, and calculate the RG-improved masses closer to the electroweak scale. But as long as the messenger scale is only a few orders of magnitude above the electroweak scale, a one-step solution to the RG equations will suffice for all parameters except B, for which a delicate cancellation occurs. The RG evolution starts at the messenger scale; it effectively stops at a typical squark mass scale $\tilde{m}$. Both of these statements were discussed and justified in Ref. [11]; in particular, the doublet and triplet messenger masses are expected to be quite similar in a unified model, so there is a reasonably well-defined single messenger scale, and most of the results do not depend significantly on the small splitting between M_{M_2} and M_{M_3}. We will usually only keep the leading powers of $L/(8\pi^2)=\ln(M_M/\tilde{m})/(8\pi^2)$, where M_M is the messenger mass scale. A more complete justification of this approximation was presented in Ref. [11]; in brief; the one-step approximation is used whenever it is sufficient, for example, in the squark masses (because their initial values are large) and in the A term [due to a cancellation of the leading $\mathcal{O}(L^2)$ effects], while higher powers of L are kept where needed, for example in Δ_t^2 of Eq. (23) and in B. Since $\tan\beta=\langle H_U\rangle/\langle H_D\rangle$ will also turn out large, we will also usually keep only leading powers of $1/\tan\beta$.

The gaugino masses, and thence the physical chargino and neutralino mass matrices, are given at the squark scale, respectively, by

$$M_i=\left(\frac{\alpha_i}{\alpha_i}\right)\hat{M}_i, \tag{9}$$

$$M_{\chi^\pm}=\begin{pmatrix} M_2 & \sqrt{2}M_W \\ 0 & \mu \end{pmatrix}, \tag{10}$$

$$M_{\chi^0}=\begin{pmatrix} M_1 & 0 & 0 & \sin\theta_W m_Z \\ 0 & M_2 & 0 & -\cos\theta_W m_Z \\ 0 & 0 & 0 & -\mu \\ \sin\theta_W m_Z & -\cos\theta_W m_Z & -\mu & 0 \end{pmatrix}. \tag{11}$$

The up- and down-type squark mass matrices $M_{\tilde{u}}^2$ and $M_{\tilde{d}}^2$, respectively, at the squark scale are

$$M_{\tilde{u}}^2=\begin{pmatrix} m_{\tilde{Q}}^2+m_u^2-\mathbf{1}\left(\frac{1}{2}-\frac{2}{3}\sin^2\theta_W\right)m_Z^2 & -m_u A_U \\ -m_u A_U & m_{\tilde{u}}^2+m_u^2-\mathbf{1}\frac{2}{3}\sin^2\theta_W m_Z^2 \end{pmatrix}, \tag{12}$$

$$M_{\tilde{d}}^2=\begin{pmatrix} m_{\tilde{Q}}^2+m_d^2+\mathbf{1}\left(\frac{1}{2}-\frac{1}{3}\sin^2\theta_W\right)m_Z^2 & \mu m_d\tan\beta \\ \mu m_d\tan\beta & m_{\tilde{d}}^2+m_d^2+\mathbf{1}\frac{1}{3}\sin^2\theta_W m_Z^2 \end{pmatrix}, \tag{13}$$

where

$$m_{\tilde{Q}}^2=\overline{m}_{\tilde{Q}}^2+\left\{\mathbf{1}\left(\frac{16}{3}g_3^2\overline{M}_3^2+3g_2^2\overline{M}_2^2+\frac{1}{15}g_1^2\overline{M}_1^2\right)-\frac{\lambda_U^2}{N}\left(\frac{16}{3}\hat{M}_3^2+3\hat{M}_2^2+\frac{13}{15}\hat{M}_1^2\right)-\frac{\lambda_D^2}{N}\left(\frac{16}{3}\hat{M}_3^2+3\hat{M}_2^2+\frac{7}{15}\hat{M}_1^2\right)\right\}\frac{L}{8\pi^2}, \tag{14}$$

$$m_{\tilde{u}}^2=\overline{m}_{\tilde{u}}^2+\left\{\mathbf{1}\left(\frac{16}{3}g_3^2\overline{M}_3^2+\frac{16}{15}g_1^2\overline{M}_1^2\right)-\frac{2\lambda_U^2}{N}\left(\frac{16}{3}\hat{M}_3^2+3\hat{M}_2^2+\frac{13}{15}\hat{M}_1^2\right)\right\}\frac{L}{8\pi^2}, \tag{15}$$

$$m_{\tilde{d}}^2=\overline{m}_{\tilde{d}}^2+\left\{\mathbf{1}\left(\frac{16}{3}g_3^2\overline{M}_3^2+\frac{4}{15}g_1^2\overline{M}_1^2\right)-\frac{2\lambda_U^2}{N}\left(\frac{16}{3}\hat{M}_3^2+3\hat{M}_2^2+\frac{7}{15}\hat{M}_1^2\right)\right\}\frac{L}{8\pi^2}. \tag{16}$$

TABLE I. The MGM predictions for μ as a function of the wino mass M_2 in the linear approximation and for some values of messenger mass M_{M_2} and top quark mass m_t, with $M_{M_3}=1.3M_{M_2}$ and $N=1$.

M_{M_2}/Λ	$m_t=165$ GeV	$m_t=175$ GeV	$m_t=185$ GeV
2	22 GeV$+1.46M_2$	23 GeV$+1.64M_2$	23 GeV$+1.82M_2$
10	22 GeV$+1.62M_2$	22 GeV$+1.81M_2$	22 GeV$+2.01M_2$
100	20 GeV$+1.70M_2$	20 GeV$+1.90M_2$	20 GeV$+2.11M_2$
1000	18 GeV$+1.74M_2$	18 GeV$+1.95M_2$	17 GeV$+2.16M_2$
10000	15 GeV$+1.76M_2$	15 GeV$+1.97M_2$	14 GeV$+2.19M_2$

$m_u(\lambda_U)$ and $m_d(\lambda_D)$ are the up- and down-type quark mass (Yukawa coupling) matrices in flavor space and A_U is given by

$$A_U=\mathbf{1}\left(\frac{16}{3}g_3^2\overline{M}_3+3g_2^2\overline{M}_2+\frac{13}{15}g_1^2\overline{M}_1\right)\frac{L}{8\pi^2}, \tag{17}$$

where the boundary condition $\overline{A}_U\simeq 0$ has been used.

For the slepton mass matrices we find, with the same approximations as for the squarks,

$$M_{\tilde{L}}^2=\begin{pmatrix} m_{\tilde{L}}^2+m_l^2+\mathbf{1}\left(\frac{1}{2}-\sin^2\theta_W\right)m_Z^2 & \mu m_l\tan\beta \\ \mu m_l\tan\beta & m_{\tilde{l}}^2+\mathbf{1}\sin^2\theta_W m_Z^2 \end{pmatrix}, \tag{18}$$

$$M_{\tilde{\nu}}^2=\left(m_{\tilde{L}}^2-\mathbf{1}\frac{1}{2}m_Z^2\right), \tag{19}$$

where

$$m_{\tilde{L}}^2=\overline{m}_{\tilde{L}}^2+\left\{\mathbf{1}\left(3g_2^2\overline{M}_2^2+\frac{3}{5}g_1^2\overline{M}_1^2\right)-\frac{\lambda_l^2}{N}\left(3\hat{M}_2^2+\frac{9}{5}\hat{M}_1^2\right)\right\}\frac{L}{8\pi^2}, \tag{20}$$

$$m_{\tilde{l}}^2=\overline{m}_{\tilde{l}}^2+\left\{\mathbf{1}\left(\frac{12}{5}g_1^2\overline{M}_1^2\right)-\frac{2\lambda_l^2}{N}\left(3\hat{M}_2^2+\frac{9}{5}\hat{M}_1^2\right)\right\}\frac{L}{8\pi^2}, \tag{21}$$

and m_l (λ_l) are the diagonal lepton mass (Yukawa) matrix in lepton flavor space.

The remaining parameters to be determined are the Higgs couplings μ and $B\mu$. These enter the scalar potential and determine the VEVs of the two Higgs doublets v_U and v_D in terms of the soft-breaking masses (discussed above) and the quartic Higgs couplings (fixed supersymmetrically by the gauge couplings). Since we are assuming $\overline{B}=0$, the only free parameter is μ, and it is set by requiring agreement with the experimental observable $v^2=v_U^2+v_D^2\simeq(174\ \text{GeV})^2$, or equivalently with $m_Z^2=(g_1^2+g_2^2)v^2/2$. Since the coupling $B\mu$ between the up- and down-type Higgs scalars will be very small, $v\simeq v_U\gg v_D$, so the electroweak scale requirement is essentially a condition on the up-type Higgs mass-squared: $m_{H_U}^2=-\frac{1}{2}m_Z^2$ to leading order. Substituting in the up-type Higgs mass as a function of μ^2, and including higher-order corrections, leads to

$$\mu^2=\lambda_t^2\Delta_t^2-m_H^2-\frac{1}{2}m_Z^2(1+\delta_H). \tag{22}$$

The details of this minimization are given in Ref. [11]: δ_H (~ 1) accounts for the loop corrections to the Higgs quartic couplings induced by the heavy top quark,

$$m_H^2\simeq\frac{1}{N}\left(\frac{3}{2}\hat{M}_2^2+\frac{3}{10}\hat{M}_1^2\right)+3\overline{g}_2^2\overline{M}_2^2\left(\frac{L}{8\pi^2}\right)$$

is the common Higgs boson mass, and $\lambda_t^2\Delta_t^2$ is the Yukawa coupling correction which lowers the up-type Higgs boson mass and breaks the electroweak symmetry. Neglecting terms smaller than $\sim 1\%$, and recalling that λ_t is evaluated at the squark mass scale as in Ref. [11], we find

$$\Delta_t^2\simeq\frac{3}{N}\frac{L_\Delta}{8\pi^2}\left\{\left[\frac{16}{3}\hat{M}_3^2+3\hat{M}_2^2\right]+\frac{L_\Delta}{8\pi^2}\times\left[N\frac{16}{3}\overline{g}_3^2\overline{M}_3^2-\left(\frac{128}{9}\overline{g}_3^2+8\overline{g}_2^2\right)\hat{M}_3^2-8\overline{g}_3^2\hat{M}_2^2\right]\right\}. \tag{23}$$

We will set the logarithm to be $L_\Delta=\ln(M_{M_3}/m_{\tilde{Q}})+3/2$ where the constant term, calculated in Ref. [27], accounts for the one-loop thresholds at the messenger scale. The absence of the complete one-loop threshold expression resulted in the major uncertainty in the previous analysis of this model [11].

Numerically, we find that μ increases approximately linearly with the superpartner scale, which we characterize by the wino mass M_2, even for light M_2. Specifically, we find that μ is given by the linear expressions of Tables I–IV for various values of N, the messenger scale and the top quark mass. These approximations yield μ within $\sim\pm 10$ GeV over the range 100 GeV$<M_2<$400 GeV. Several features are evident in these results: μ increases with the messenger scale and with the top quark mass, since it must cancel a larger radiative correction $\lambda_t^2\Delta_t^2$; it decreases with N relative to M_2, since more messengers lower the sfermions relative to the gauginos [see Eqs. (1),(2)] and it is rather insensitive to small messenger splittings induced presumably by RG evolution from high scales.

TABLE II. The MGM predictions for μ as a function of the wino mass M_2 in the linear approximation and for some values of messenger mass M_{M_3} and top quark mass m_t, with $M_{M_2}=1.3M_{M_3}$ and $N=1$.

M_{M_3}/Λ	$m_t=165$ GeV	$m_t=175$ GeV	$m_t=185$ GeV
2	21 GeV$+1.43M_2$	21 GeV$+1.61M_2$	21 GeV$+1.80M_2$
10	21 GeV$+1.57M_2$	21 GeV$+1.76M_2$	20 GeV$+1.96M_2$
100	19 GeV$+1.66M_2$	19 GeV$+1.86M_2$	19 GeV$+2.07M_2$
1000	17 GeV$+1.71M_2$	17 GeV$+1.91M_2$	16 GeV$+2.12M_2$
10000	15 GeV$+1.73M_2$	15 GeV$+1.94M_2$	14 GeV$+2.15M_2$

Finally, $\tan\beta=v_U/v_D$ is predicted by minimizing the full scalar potential for both Higgs doublets:

$$\frac{1}{\tan\beta}=-\frac{B\mu}{m^2_{\mathrm{eff},A}}. \tag{24}$$

A striking aspect of the MGM is that, assuming $\overline{B}=0$ (or practically zero), the low-energy value of B is also very small, and hence $\tan\beta$ is naturally very large [6,11] (see also the last reference in Ref. [15]). The reason is not simply a small amount of RG evolution between the messenger and squark mass scales, but rather [11] a cancellation between the direct gaugino contribution to the RG evolution and the direct A-term (or indirect gluino) contribution to that evolution — a fortuitous cancellation that happens when M_M is not too far above its minimal value Λ. Thus if the messengers are not too heavy, the B parameter evaluated at the squark mass scale is very small, as it is at the messenger scale, although for intermediate scales B is considerably larger. So the coupling between the Higgs scalars is predicted to be very small at the relevant scale of electroweak breaking, which leads to a large hierarchy between their VEVs: $\tan\beta=v_U/v_D\gg 1$. Because of the cancellation of the leading-order terms, the $B(m_{\tilde{Q}})$ must be calculated quite carefully at the next-to-leading order. The analytic results of this calculation, and the expression for the effective pseudoscalar mass-squared parameter $m^2_{\mathrm{eff},A}$ to be used in minimizing the potential, are given in Ref. [11]. Then $\tan\beta$ is predicted by solving Eq. (24) numerically, taking into account the implicit dependence of the right-hand side (and in particular of B) on $\tan\beta$.

In addition to new mass scale parameters, the MSSM is characterized by two new phase parameters beyond the SM. The MGM predicts these signs in any fixed convention. To see this, note that they may be put entirely into the A and B parameters by appropriate field redefinitions [28]. But in minimal gauge mediation the A and B parameters of the effective MSSM at the messenger scale vanish, and hence the phase parameters are predicted: they vanish. Then their values at lower scales follow from the calculable RG evolution of A and B. In a convention where the gaugino masses and top and bottom Yukawa couplings are real, no complex phases can then be generated (at least in low orders) in A and B, only a relative sign, which we calculate below.

This sign is particularly crucial for the observables of interest to us, $g_\mu-2$ and $b\to s\gamma$, which are enhanced by large $\tan\beta$. As shown in the second reference of Ref. [13], all such observables proportional to $\tan\beta$ are also proportional to the degree of breaking of the Peccei-Quinn (PQ) symmetry of the Higgs sector, characterized by μ, and of an R symmetry, characterized by the gaugino mass $M_{1/2}$. The amplitudes of these observables will be determined by the sign of the product $\tan\beta\mu M_{1/2}$, which is a prediction of the MGM in any fixed Lagrangian convention, as we calculate below. The final predictions of the observables will of course be independent of any convention.

To state the sign, we must establish some convention. In two-component Weyl notation, we use a Lagrangian schematically of the form

$$\mathcal{L}_{\mathrm{gauge}}\sim ig(\tilde{G}t_L\tilde{t}_L-\tilde{G}t_R\tilde{t}_R), \tag{25}$$

$$\mathcal{L}_{\mathrm{Yukawa}}\sim-\int d^2\theta W,\quad W\sim\mu H^0_U H^0_D+\lambda_t H^0_U t_L t_R, \tag{26}$$

$$\mathcal{L}_{\mathrm{soft}}\sim-M_{1/2}\tilde{G}\tilde{G}-\lambda_t A_t\tilde{t}_L\tilde{t}_R H^0_U-B\mu H^0_U H^0_D, \tag{27}$$

$$\mathcal{L}_{\mathrm{F}}\sim-|\partial W/\partial\phi|^2\sim-\lambda_t\mu H^0_D\tilde{t}_L\tilde{t}_R. \tag{28}$$

Here $H^0_{U,D}$ are the neutral components of the Higgs doublets, $\tilde{G}$ is the gaugino field, and the proper group structure and

TABLE III. The μ MGM predictions as in Table I with $N=2$

M_{M_2}/Λ	$m_t=165$ GeV	$m_t=175$ GeV	$m_t=185$ GeV
2	8 GeV$+1.10M_2$	9 GeV$+1.23M_2$	10 GeV$+1.36M_2$
10	9 GeV$+1.23M_2$	10 GeV$+1.37M_2$	11 GeV$+1.51M_2$
100	9 GeV$+1.31M_2$	10 GeV$+1.46M_2$	10 GeV$+1.60M_2$
1000	8 GeV$+1.35M_2$	9 GeV$+1.50M_2$	9 GeV$+1.65M_2$
10000	7 GeV$+1.37M_2$	8 GeV$+1.53M_2$	8 GeV$+1.68M_2$

TABLE IV. The μ MGM predictions as in Table II for $N=2$.

M_{M_3}/Λ	$m_t=165$ GeV	$m_t=175$ GeV	$m_t=185$ GeV
2	6 GeV$+1.08M_2$	7 GeV$+1.21M_2$	8 GeV$+1.34M_2$
10	7 GeV$+1.19M_2$	9 GeV$+1.33M_2$	9 GeV$+1.47M_2$
100	8 GeV$+1.27M_2$	9 GeV$+1.42M_2$	9 GeV$+1.56M_2$
1000	7 GeV$+1.32M_2$	8 GeV$+1.47M_2$	8 GeV$+1.62M_2$
10000	6 GeV$+1.34M_2$	7 GeV$+1.50M_2$	7 GeV$+1.65M_2$

indices are implied: our purpose is only to establish the sign convention. With this Lagrangian, we calculate (and find agreement with Moroi [22]) that, for example, the dominant MSSM contribution to $g_\mu-2$ is $\Delta a\sim+M_{1/2}\mu\tan\beta$. We can also easily extract and minimize the scalar Higgs potential to find $1/\tan\beta\sim-B\mu$. Next, a one-loop top-gluino diagram using this Lagrangian generates $A_t\sim+M_{1/2}$. Then B is generated by both a one-loop top squark diagram with an A insertion, $B_A\sim-A_t\sim-M_{1/2}$, and a one-loop Higgsino–W-ino diagram, $B_G\sim+M_{1/2}$. The coincidental near cancellation of these two is the reason $\tan\beta$ is large in the MGM, but we find that essentially always $|B_A|>|B_G|$, so $B\sim-M_{1/2}$. Therefore with this sign convention $M_{1/2}\mu\tan\beta>0$. Hence the *convention-independent*, *physical* sign of Δa is positive, and similarly the deviations of the various $b\to s\gamma$ amplitudes are unambiguously predicted.

To be more specific, for the remainder of this paper we will further specify that μ and $M_{1/2}$ are positive, and therefore so is $\tan\beta$. To translate our intermediate results to different Lagrangian conventions, the interested reader need only use the Lagrangian of Eqs. (25)–(28) to determine the desired signs of μ and $M_{1/2}$, and then establish the corresponding sign of $\tan\beta$ from $M_{1/2}\mu\tan\beta>0$. Our final results are physical, and therefore will be unchanged. In much of the existing literature, the signs of $M_{1/2}$ and $\tan\beta$ are fixed by convention, in which case the MGM makes a prediction of the sign of μ.

We conclude this section by observing that the low-energy mass spectrum in the MSSM, as well as $\tan\beta$ and the sign of μ, can be predicted within the MGM in terms of only the SUSY-breaking scale Λ (or equivalently any particular superpartner mass, say the W-ino M_2) and the logarithm of the messenger mass scale M_M. This extraordinary predictivity forms the basis for the remainder of this work: the formulation of low-energy experimental tests of the MGM.

III. b→sγ

As discussed in the previous section, an interesting feature of the MGM model is that $\tan\beta$ is predicted large. Since we are interested in constraining this model from low-energy physics, we will restrict our investigation to some processes which are particularly sensitive to large $\tan\beta$ values. It is well known that the low-energy processes mediated by magnetic dipole transitions can be significantly enhanced in the MSSM for $\tan\beta\gg1$, because the chiral suppression of superpartner-mediated diagrams is removed to a large extent by the large $\tan\beta$ (i.e., the Yukawa couplings are no longer small), which allows for a competition with the chirally suppressed SM amplitude. Among this class of processes we consider here the rare $B\to X_s\gamma$ decay. In particular in this section we will give the analytical results for the dominant contributions to the $B\to X_s\gamma$ decay in the MGM model, and fold them in with the recent next to leading order (NLO) calculation for the SM.

Let us start with the experimental results. The most recent published result by the CLEO Collaboration for the total *inclusive* branching ratio $\mathrm{BR}(B\to X_s\gamma)$ is [29]

$$10^4\times\mathrm{BR}^{\mathrm{expt}}(B\to X_s\gamma)=2.32\pm0.67 \tag{29}$$

combining 1 σ uncertainties and

$$1.0<10^4\times\mathrm{BR}^{\mathrm{expt}}(B\to X_s\gamma)<4.2 \tag{30}$$

at the 95% confidence level.

Recently the NLO corrections to the quark $b\to s\gamma$ decay rate have been completed in Ref. [24], including the calculation of the three-loop anomalous dimension matrix of the effective theory. This is a necessary ingredient for a consistent resummation, at the NLO accuracy, of the large leading logarithms, $\log M_W/m_b$.

The inclusion of the NLO corrections in the $b\to s\gamma$ decay rate has significantly reduced the large theoretical uncertainty present in the previous LO calculation. From the quark-level $b\to s\gamma$ decay rate it is possible to infer the B meson *inclusive* branching ratio $\mathrm{BR}_\gamma\equiv\mathrm{BR}(B\to X_s\gamma)$ by including the small (percent-level) nonperturbative $1/m_b$ [30] and $1/m_c$ [31,32] corrections. The result, the most recent theoretical prediction for $\mathrm{BR}_\gamma^{\mathrm{NLO}}$ in the SM is [33]

$$10^4\mathrm{BR}_\gamma^{\mathrm{NLO}}=3.48\pm0.31, \tag{31}$$

where the theoretical uncertainty, $\sim10\%$, is less than half the previous LO uncertainty. It includes the uncertainty in the SM input parameters m_t, $\alpha_s(M_Z)$, α_{em}, m_c/m_b, m_b, CKM angles, and the residual scale dependence uncertainties. Nevertheless the error is dominated by the uncertainty on the SM input parameters, as claimed in Ref. [33]. Comparing with the experimental result in Eq. (29), the SM prediction is higher than the observed branching ratio, although the disagreement is less than two experimental standard deviations.

To compute the deviations expected in the MGM, we look closer at the theoretical calculation. The nonleptonic low-energy effective Hamiltonian $H_{\mathrm{eff}}^{\mathrm{NL}}$ relevant for the $b\to s\gamma$ decay is

$$H_{\rm eff}^{\rm NL}=-\frac{4G_F}{\sqrt{2}}V_{ts}^*V_{tb}\sum_{i=1}^{8}C_i(\mu_b)Q_i(\mu_b), \tag{32}$$

where V_{ij} are the Cabibbo-Kobayashi-Maskawa (CKM) matrix elements, $C_i(\mu_b)$ the Wilson coefficients, and $Q_i(\mu_b)$ the corresponding operators evaluated at the renormalization scale $\mu_b\simeq\mathcal{O}(m_b)$. Only the magnetic and chromomagnetic dipole operators Q_7 and Q_8, respectively, are significantly affected by new MGM amplitudes; their expressions are given by

$$Q_7=\frac{e}{16\pi^2}m_b(\bar{s}_L\sigma^{\mu\nu}b_R)F_{\mu\nu}, \tag{33}$$

$$Q_8=\frac{g_s}{16\pi^2}m_b(\bar{s}_L\sigma^{\mu\nu}T^a b_R)G^a_{\mu\nu}, \tag{34}$$

where T^a are the $\mathrm{SU}(3)_{\rm color}$ generators and $F_{\mu\nu}$ and $G^a_{\mu\nu}$ are, respectively, the electromagnetic and $\mathrm{SU}(3)_{\rm color}$ field strengths with e and g_s the corresponding coupling constants. The remaining operators in the complete basis can be found in Ref. [24] or [33]. The Wilson coefficients $C_i(\mu)$, which satisfy the RG equation

$$\mu\frac{d}{d\mu}C_i(\mu)=C_j(\mu)\gamma_{ji}(\mu), \tag{35}$$

can be expanded, together with the anomalous dimension matrix γ_{ij}, in powers of α_s as follows:

$$\hat{\gamma}=\frac{\alpha_s(\mu)}{4\pi}\hat{\gamma}^{(0)}+\frac{\alpha_s^2(\mu)}{(4\pi)^2}\hat{\gamma}^{(1)}+\mathcal{O}(\alpha_s^3), \tag{36}$$

$$C_i(\mu)=C_i^{(0)}(\mu)+\frac{\alpha_s(\mu)}{4\pi}C_i^{(1)}(\mu)+\mathcal{O}(\alpha_s^2). \tag{37}$$

Then the solution in the modified minimal subtraction ($\overline{\rm MS}$) renormalization scheme for $\mu=\mu_b$ is given by

$$C_7^{(0)}(\mu_b)=\eta^{16/23}C_7^{(0)}(M_W)+\frac{8}{3}(\eta^{14/23}-\eta^{16/23})C_8^{(0)}(M_W)+\sum_{i=1}^{8}h_i\eta^{a_i}, \tag{38}$$

$$\begin{aligned}C_7^{(1)}(\mu_b)=&\eta^{39/23}C_7^{(1)}(M_W)+\frac{8}{3}(\eta^{37/23}-\eta^{39/23})C_8^{(1)}(M_W)\\&+\left(\frac{297664}{14283}\eta^{16/23}-\frac{7164416}{357075}\eta^{14/23}+\frac{256868}{14283}\eta^{37/23}-\frac{6698884}{357075}\eta^{39/23}\right)C_8^{(0)}(M_W)\\&+\frac{37208}{4761}(\eta^{39/23}-\eta^{16/23})C_7^{(0)}(M_W)+\sum_{i=1}^{8}[e_i\eta E(x_t)+f_i+g_i\eta]\eta^{a_i},\end{aligned} \tag{39}$$

where $\eta=\alpha_s(M_W)/\alpha_s(\mu_b)$, $x_t=m_t^2/M_W^2$, and α_s is calculated at NLO. The SM contribution to $C_{7,8}^{(0,1)}(M_W)$ together with the real numbers a_i, f_i, g_i, h_i, and the function $E(x)$ can be found in Ref. [24].

Finally the branching ratio BR_γ, conventionally normalized to the semileptonic branching ratio $\mathrm{BR}(B\to X_c e\nu)=(10.4\pm0.4)\%$ [34], is given by [24]

$$\begin{aligned}\mathrm{BR}_\gamma^{\rm NLO}=&BR(B\to X_c e\nu)\frac{|V_{ts}^*V_{tb}|^2}{|V_{cb}|^2}\frac{6\alpha_{\rm em}}{\pi g(z)k(z)}\\&\times\left(1-\frac{8}{3}\frac{\alpha_s(m_b)}{\pi}\right)(|D|^2+A)(1+\delta_{np}),\end{aligned}$$

$$\begin{aligned}D=&C_7^{(0)}(\mu_b)+\frac{\alpha_s(\mu_b)}{4\pi}\\&\times\left(C_7^{(1)}(\mu_b)+\sum_{i=1}^{8}C_i^{(0)}(\mu_b)\left[r_i(z)+\gamma_{i7}^{(0)}\log\frac{m_b}{\mu_b}\right]\right),\end{aligned}$$

$$\begin{aligned}A=&(e^{-\alpha_s(\mu_b)\log\delta(7+2\log\delta)/3\pi}-1)|C_7^{(0)}(\mu_b)|^2\\&+\frac{\alpha_s(\mu_b)}{\pi}\sum_{i,j=1}^{8}C_i^{(0)}(\mu_b)C_j^{(0)}(\mu_b)f_{ij}(\delta),\end{aligned} \tag{40}$$

where $z=m_c^2/m_b^2$ and in the last sum $i\leqslant j$. The expressions for all LO Wilson coefficients $C_i^{(0)}(\mu_b)$ together with the functions $g(z)$, $k(z)$, $r_i(z)$, and $f_{ij}(\delta)$ can be found in Ref. [24]. The term $\delta_{\rm np}$, of order a few percent, includes the nonperturbative $1/m_b$ [30], and $1/m_c$ [31,32] corrections.

Some comments about this result are in order.

(1) With NLO accuracy the inclusive $b\to s\gamma$ decay rate is given by the sum of the total rate for $b\to s\gamma$ decay and its gluon bremsstrahlung corrections $b\to s\gamma g$, where in the former the $\mathcal{O}(\alpha_s)$ radiative corrections to the matrix element are included and in the latter an explicit lower cut on the photon energy resolution $E_\gamma>(1-\delta)m_b/2$ is made. In the sum of these two contributions the only remaining infrared cutoff is the logarithm of δ in the A term of Eq. (40).

(2) The LO result can easily be recovered by taking the limit of $\alpha_s\to0$ inside the expression for the D and A terms.

(3) To retain a strictly NLO result, the terms proportional to α_s^2 in the $|D|^2$ expression should be discarded.

Since the new physics scale is above the electroweak scale, the new contributions to the $b\to s\gamma$ decay will affect only the SM Wilson coefficients at the M_W scale. Therefore the nonperturbative resummation of the large logarithms from M_W to μ_b can be taken completely from the existing

SM calculation. Of course this would not hold if there were new operators, generated at the electroweak scale, which would significantly correct $C_7(\mu_b)$ via mixing with Q_7. But in the MGM this does not occur: the dominant contributions to the $b\to s\gamma$ decay enter only in the Wilson coefficients $C_7(M_W)$ and $C_8(M_W)$. We define fractional deviations $R_{7,8}$ from the SM amplitudes

$$C_{7,8}^{(0)}(M_W)\equiv C_{7,8}^{(0)\mathrm{SM}}(M_W)(1+R_{7,8}), \tag{41}$$

where $C_i^{(0)\mathrm{SM}}(M_W)$ represent the LO SM contribution. Inserting these definitions into the BR_γ formula in Eq. (40) yields a general parametrization of the branching ratio in terms of the new contributions [35]:

$$10^4\mathrm{BR}_\gamma^{\mathrm{NLO}}=(3.48\pm 0.31)(1+0.622R_7+0.090R_7^2+0.066R_8 +0.019R_7R_8+0.002R_8^2), \tag{42}$$

where the following central values are used:

$$m_t^{\mathrm{pole}}\simeq \overline{m_t^{\mathrm{MS}}}(m_Z)\simeq 174\ \mathrm{GeV},\ \ m_b^{\mathrm{pole}}=4.8\ \mathrm{GeV},$$

$$m_c^{\mathrm{pole}}=1.3\ \mathrm{GeV},\ \ \mu_b=m_b,\ \ \alpha_s(m_Z)=0.118,$$

$$\alpha_{\mathrm{em}}^{-1}(m_Z)=128,\ \ \sin^2\theta_W=0.23,$$

and a photon energy resolution corresponding to $\delta=0.9$ is assumed.

What are the contributions to $R_{7,8}$ in the MGM model? In general in the MSSM the diagrams which contribute to the $b\to s\gamma$ amplitude, in addition to the SM, are given by a chargino, neutralino, gluino and charged Higgs boson exchange.

The charged Higgs-boson-exchange amplitude ($\mathcal{A}_{H^-}$) is well-known to be large [12,13,15]. More recently it was pointed out that for large $\tan\beta$ also the chargino and gluino exchange can give sizeable contributions to the $b\to s\gamma$ amplitude [13]. In particular, the leading large $\tan\beta$ contributions to the amplitude arise from exchanges of a pure Higgsino ($\mathcal{A}_{\tilde h^-}$), a mixed W-ino–Higgsino ($\mathcal{A}_{\tilde W\tilde h^-}$), or a gluino ($\mathcal{A}_{\tilde g}$), in descending order of importance. Thus

$$R_7=\frac{\mathcal{A}_{H^-}+\mathcal{A}_{\tilde h^-}+\mathcal{A}_{\tilde W\tilde h^-}+\mathcal{A}_{\tilde g}}{\mathcal{A}_{\mathrm{SM}}}, \tag{43}$$

where the amplitude $\mathcal{A}_{\mathrm{SM}}$ correspond to an exchange of a W boson. We stress here that the same mechanism of $\tan\beta$ enhancement is present also in the $\delta m_b/m_b$ radiative corrections to the bottom quark masses [13]. Indeed the diagrams contributing to the $b\to s\gamma$ amplitude are the same as for $\delta m_b/m_b$, but where a photon line is attached in all possible ways. Also, as explained above, the MSSM contributions are proportional to the relative sign of μ, $M_{1/2}$, and $\tan\beta$. In the MGM this sign is calculable, and therefore a unique prediction of $b\to s\gamma$ decay rate in terms of only the messenger and gaugino mass can be given [11,35].

In the MSSM the complete and exact analytical results for the $b\to s\gamma$ and $b\to sg$ total amplitudes can be found in Ref. [12], in terms of the various mass eigenvalues. However, since in the MGM the squarks are quite heavy, a mass insertion approximation will suffice [11]. Here we diagonalize the chargino mass matrix exactly, since we are interested in light charginos. The result for the partial amplitudes is, up to an overall normalization [35],

$$\mathcal{A}_{\mathrm{SM}}=\frac{3}{2}V_{ts}x_{tW}\left[\frac{2}{3}F_1(x_{tW})+F_2(x_{tW})\right], \tag{44}$$

$$\mathcal{A}_{\mathrm{H}^-}=\frac{1}{2}V_{ts}r_b x_{tH}\left[\frac{2}{3}F_3(x_{tH})+F_4(x_{tH})\right], \tag{45}$$

$$\mathcal{A}_{\tilde{\mathrm{h}}^-}=\frac{1}{2}V_{ts}r_b\tan\beta\frac{\mu m_t m^2_{\tilde t_L\tilde t_R}}{m^2_{\tilde t_L}m^2_{\tilde t_R}} \times\left[M_2^2\frac{F(x_{\tilde h_1\tilde t},x_{\tilde h_2\tilde t})}{M^2_{\tilde h_1^-}-M^2_{\tilde h_2^-}}-|m_{\tilde t_L}m_{\tilde t_R}|\frac{F'(x_{\tilde h_1\tilde t},x_{\tilde h_2\tilde t})}{M^2_{\tilde h_1^-}-M^2_{\tilde h_2^-}}\right], \tag{46}$$

$$\mathcal{A}_{\tilde{\mathrm{W}}\tilde{\mathrm{h}}^-}=r_b\tan\beta\frac{m_W^2m^2_{\tilde t_L\tilde c_L}}{m^2_{\tilde t_L}m^2_{\tilde c_L}}\mu M_2\frac{F(x_{\tilde h_1\tilde q_L},x_{\tilde h_2\tilde q_L})}{M^2_{\tilde h_1^-}-M^2_{\tilde h_2^-}}, \tag{47}$$

$$\mathcal{A}_{\tilde{\mathrm{g}}}=\frac{8}{9}r_b\tan\beta\frac{\alpha_s}{\alpha_W}\frac{m_W^2m^2_{\tilde t_L\tilde c_L}\mu M_3}{m^6_{\tilde q}}F_{\mathrm{gl}}(x_{M_3\tilde q}), \tag{48}$$

where $r_b\equiv 1/(1+\delta m_b/m_b)$ accounts for the mass corrections to m_b [11]. The functions F_i can be found in Ref. [12], while the new functions are defined as follows:

$$F(x_1,x_2)=f(x_1)-f(x_2),\quad F'(x_1,x_2)=x_1f(x_1)-x_2f(x_2), \tag{49}$$

$$f(x)\equiv\frac{d}{dx}\left(xF_3+\frac{2}{3}xF_4\right),\quad F_{\mathrm{gl}}(x)\equiv\frac{1}{2}\frac{d^2}{dx^2}(x^2F_4). \tag{50}$$

We also use

$$x_{tW}=\frac{m_t^2}{m_W^2},\quad x_{tH}=\frac{m_t^2}{m^2_{H^-}},\quad x_{\tilde h_i\tilde t}=\frac{M^2_{\tilde h_i^-}}{|m_{\tilde t_L}m_{\tilde t_R}|}, \tag{51}$$

$$x_{\tilde h_i\tilde q_L}=\frac{M^2_{\tilde h_i^-}}{|m_{\tilde t_L}m_{\tilde c_L}|},\quad x_{M_3\tilde q}=\frac{M_3^2}{m^2_{\tilde q}}, \tag{52}$$

where $M_{\tilde h_i^-}$ is the ith chargino mass eigenvalue and $m_{\tilde q}$ is the average squark mass. The left-right top squark mass insertion is $m^2_{\tilde t_L\tilde t_R}=m_tA_t$ (>0), while the left-left top squark scharm mass insertion is given by [11]

$$m^2_{\tilde{t}_L\tilde{c}_L} \simeq + V_{ts} m^2_{\tilde{q}} \frac{\lambda_t^2}{4\pi^2} \ln\left(\frac{M_M}{m_{\tilde{t}}}\right). \tag{53}$$

The contribution to R_8 can be obtained from Eq. (43) after the following replacement in the amplitudes of Eqs. (44)–(48):

$$\frac{2}{3}F_1 + F_2 \to F_1, \quad \frac{2}{3}F_3 + F_4 \to F_3, \quad f \to \frac{d}{dx}(xF_4), \tag{54}$$

$$F_{\rm gl}(x) \to \frac{9}{16}\frac{d^2}{dx^2}\left(3x^2F_3 + \frac{1}{3}x^2F_4\right). \tag{55}$$

At present in the MSSM the supersymmetric corrections to $C_7(M_W)$ and $C_8(M_W)$ are known only at LO; we will return to comment on the resultant uncertainties when we present the numerical predictions for BR_γ decay, in terms of the SUSY breaking scale and the messenger mass scale M_M, in Sec. VI.

IV. $b \to s\ell^+\ell^-$

In this section we consider the semileptonic flavor-changing decays $b \to s e^+ e^-$, $b \to s \mu^+ \mu^-$, and $b \to s \tau^+ \tau^-$. These processes are interesting for several reasons: first, they are sensitive to new physics with large $\tan\beta$ for the same reason that $b \to s\gamma$ is sensitive, and in fact because of the same operator Q_7 (see also Ref. [18]). Second, they involve other operators as well, and so can serve as complementary tests of the model [36]. Third, since there are several measurable quantities (branching ratios and asymmetries in several systems), they can potentially yield much more data. At present these decays are known at the NLO logarithmic accuracy for the SM [25,26]. The $1/m_b$ nonperturbative contributions are small and well under control, except near the end-point of the dilepton mass spectrum [37]. Recently it was pointed out that other nonperturbative power corrections $\mathcal{O}(\Lambda^2_{QCD}/m_c^2)$ could affect the amplitude, but in practice they are very small [32]. Moreover there are other nonperturbative effects due to the resonance regions in the dilepton invariant mass distribution. But these do not have to be taken into account if certain regions are excluded from the integration region.

Unfortunately, the expected branching ratio for these decays is too small to be observed in present experiments. The SM predictions for the nonresonant decay rates $\mathrm{BR}(b \to s\ell^+\ell^-) \equiv \mathrm{BR}_{\ell\ell}$ are given by [16,35]

$$\mathrm{BR}_{ee} \simeq 7.0 \times 10^{-6}, \tag{56}$$

$$\mathrm{BR}_{\mu\mu} \simeq 4.5 \times 10^{-6}, \tag{57}$$

$$\mathrm{BR}_{\tau\tau} \simeq 2.0 \times 10^{-7}; \tag{58}$$

at present, experiments only place some upper bounds on BR_{ee} and $\mathrm{BR}_{\mu\mu}$, $\mathcal{O}(\mathrm{few} \times 10^{-5})$, or about an order of magnitude above the SM [38]. However, an increase of two to four orders of magnitude in the experimental sensitivity is expected in the near future at the Tevatron [39]. With such statistics it will be possible to measure the branching ratio and the energy or angular distributions, even for the more rare τ decay mode.

We now turn to our prediction for the branching ratios and asymmetries. The effective Hamiltonian $H_{\rm eff}$ relevant for the $b \to s\ell^+\ell^-$ decay is

$$H_{\rm eff} = H_{\rm eff}^{\rm NL} - \frac{G_F}{\sqrt{2}} V_{ts}^* V_{tb} \{C_9(\mu_b) Q_9(\mu_b) + C_{10}(\mu_b) Q_{10}(\mu_b)\}, \tag{59}$$

where $H_{\rm eff}^{\rm NL}$ is given in Eq. (32) with $\mu_b \simeq \mathcal{O}(m_b)$, the magnetic-dipole operator Q_7 is defined in Eq. (33), and the semileptonic operators Q_9 and Q_{10} are given by

$$Q_9 = [\bar{s}\gamma^\mu(1-\gamma_5)b](\bar{l}\gamma^\mu l), \tag{60}$$

$$Q_{10} = [\bar{s}\gamma^\mu(1-\gamma_5)b](\bar{l}\gamma^\mu\gamma_5 l). \tag{61}$$

The Wilson coefficients $C_9(\mu_b)$ and $C_{10}(\mu_b)$ at NLO are

$$C_9(\mu_b) = \frac{\alpha}{2\pi}[P_0(\mu_b, \eta) + P_E E] + C_9(M_W), \tag{62}$$

where the initial conditions $C_{9,10}(M_W)$ in the HV scheme are given by [26]

$$C_9(M_W) = \frac{\alpha}{2\pi}\left(\frac{1}{\sin^2\theta_W} Y - 4Z\right) \tag{63}$$

$$C_{10}(\mu_b) = C_{10}(M_W) = -\frac{\alpha}{2\pi \sin^2\theta_W} Y. \tag{64}$$

The terms Y, Z, and E contain the results of the one-loop integration for the γ, Z penguin and box diagrams at the electroweak scale. The SM expressions for Y, Z, E, respectively the functions $Y^{\rm SM}(x_t)$, $Z^{\rm SM}(x_t)$, and $E^{\rm SM}(x_t)$ $(x_t = m_t^2/M_W^2)$, can be found in Refs. [25,26]. The function P_0 includes the resummation of the large logarithms at the NLO and it is scheme dependent. Finally, in the limit $\eta \to 1$, $P_E \to 0$ and $P_0 \to 0$, so that the initial condition $C_9(\mu) \to C_9(M_W)$ is recovered. The expressions for P_0 and P_E, in both HV and NDR scheme for the former, can be found in Ref. [26].

Note that $C_{10}(\mu_b)$ does not actually depend on the renormalization scale μ_b. This can be understood as follows. Since the $\bar{s}\gamma_\mu(1-\gamma_5)b$ current is not renormalized, Q_{10} does not contribute to its own anomalous dimension (the same holds for Q_9) and due to the P and C symmetry of the electromagnetic current, there are also no contributions to its anomalous dimension from mixing with Q_9 or any nonleptonic operators of Eq. (32).

At NLO accuracy the total amplitude for $b \to s\ell^+\ell^-$ decay can be expressed as a function of $C_9^{\rm eff}(\mu_b) = C_9(\mu_b) + C_9^{\rm ME}(\mu_b)$, $C_7^{(0)}(\mu_b)$, and $C_{10}(M_W)$ where $C_9^{\rm ME}(\mu_b)$ con-

tains the $\mathcal{O}(\alpha_s)$ one-loop matrix elements needed to cancel the leading μ_b dependence in $C_9(\mu_b)$. Moreover $C_9^{\rm eff}$ is scheme independent since $C_9^{\rm ME}$ cancels exactly the scheme dependence of $C_9(\mu_b)$ [26]. Note that at NLO accuracy, $C_7(\mu_b)$ enter only at the leading order.

Finally the differential decay rate for $b\to s\ell^+\ell^-$ is given by

$$\frac{d^2\Gamma_{\ell\ell}}{dy_+dy_-}=\frac{G_F^2}{256\pi^5}m_b^5|V_{ts}^*V_{tb}|^2\alpha_{\rm em}^2\{|C_9^{\rm eff}(\mu_b)|^2K^{9,9}+C_{10}^2(M_W)K^{10,10}+[C_7^{(0)}(\mu_b)]^2K^{7,7}+C_7^{(0)}(\mu_b){\rm Re}[C_9^{\rm eff}(\mu_b)]K^{7,9}+C_{10}(M_W)\times(C_7^{(0)}(\mu_b)K^{7,10}+{\rm Re}[C_9^{\rm eff}(\mu_b)]K^{9,10})\}. \tag{65}$$

Note that $C_7^{(0)}(\mu_b)$ is real [see Eq. (38)] as is $C_{10}(M_W)$, while $C_9^{\rm eff}(\mu_b)$ is complex — its imaginary part originates in the one-loop matrix elements in $C_9^{\rm ME}(\mu_b)$. The kinematic variables are $y_\pm=2E_\pm/m_b$ where $E_\pm$ are the lepton energies measured in the b rest frame. We prefer to use the following combinations:

$$\hat{s}=y_++y_--1, \tag{66}$$

$$\hat{y}=y_+-y_-=-\hat{y}_{\rm max}\cos\theta,$$

where $\hat{y}_{\rm max}=(1-\hat{s})\sqrt{1-4x_\ell/\hat{s}}$, $x_\ell=m_\ell^2/m_b^2$, and θ is the angle between the b and the ℓ^+ in the $\ell^+\ell^-$ rest frame. Including only the lepton mass corrections, we find

$$K^{9,9}=\frac{1}{2}[1-\hat{s}^2-\hat{y}^2+4x_\ell(1-\hat{s})], \tag{67}$$

$$K^{10,10}=\frac{1}{2}[1-\hat{s}^2-\hat{y}^2-4x_\ell(1-\hat{s})], \tag{68}$$

$$K^{7,7}=\frac{2}{\hat{s}}\left[1-\hat{s}^2+\hat{y}^2+\frac{4x_\ell}{\hat{s}}(1-\hat{s})\right], \tag{69}$$

$$K^{7,9}=4\left[1-\hat{s}+\frac{2x_\ell}{\hat{s}}(1-\hat{s})\right], \tag{70}$$

$$K^{7,10}=4\hat{y}, \tag{71}$$

$$K^{9,10}=2\hat{s}\hat{y}. \tag{72}$$

The results of Eqs. (65),(67)–(72) are in agreement with Ref. [16], where the massless case is considered. Moreover, after integrating Eq. (65) with respect to $\hat{y}$, our result agrees with that of Ref. [19], including the mass corrections.

The $1/\hat{s}$ terms present in Eqs. (69),(70) are due to the photon propagator which connects the quark matrix element of the magnetic dipole operator Q_7 to the electromagnetic lepton current. As observed in Ref. [16] the last term of Eq. (69) proportional to the lepton mass (x_ℓ) cannot be completely neglected even in the light lepton case. In particular it gives a finite contribution to the total branching ratio (roughly a few per cent) even in the $m_l^2\to 0$ limit. Indeed the $1/\hat{s}^2$ term in Eq. (69) generates a pole $\mathcal{O}(1/m_l^2)$ in the integrated branching ratio which is cancelled by the $\mathcal{O}(m_l^2)$ terms present in the numerator.

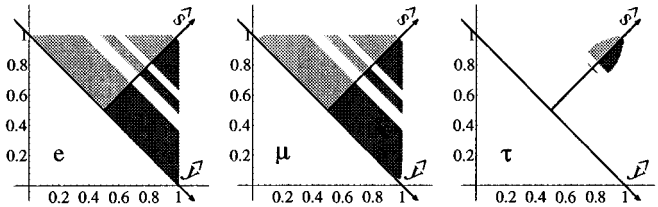

FIG. 1. Dalitz plots for the integrating regions of $b\to s\ell^+\ell^-$ decays corresponding to e, μ, and τ decay modes from the left to the right.

The total branching ratio for a particular ℓ is obtained integrating $d^2\Gamma_{\ell\ell}/dy_+dy_-$ over the entire kinematically allowed range for that ℓ. The forward-backward asymmetry $A_{\ell\ell}$ (which is the same as the energy asymmetry) is proportional to the integral over the range $y_->y_+$ (i.e., $\cos\theta>0$) minus the integral over the range $y_-<y_+$ ($\cos\theta<0$). The allowed kinematic limits are $-\hat{y}_{\rm max}<\hat{y}<+\hat{y}_{\rm max}$ and $4x_\ell<\hat{s}<1$.

To avoid intermediate charmonium resonances and nonperturbative phenomena near the end point, we exclude the same ranges of $\hat{s}$ specified in Ref. [16]. In particular, the integrating regions of $\hat{s}$ in the $l=e,\mu$ case are

$$(m_b^2\hat{s})\in\{4m_l^2,\ (2.9\ {\rm GeV})^2\}\cup\{(3.3\ {\rm GeV})^2,\ (3.6\ {\rm GeV})^2\}\cup\{(3.8\ {\rm GeV})^2,\ (4.6\ {\rm GeV})^2\} \tag{73}$$

and for $l=\tau$

$$(m_b^2\hat{s})\in\{4m_\tau^2,\ (3.6\ {\rm GeV})^2\}\cup\{(3.8\ {\rm GeV})^2,\ (4.6\ {\rm GeV})^2\}. \tag{74}$$

The Dalitz plots for the decays $b\to s\ell^+\ell^-$ are shown in Fig. 1. The dimensionless lepton energies y^+ and y^- run along the horizontal and vertical axes, respectively. The rotated axes correspond to $\hat{y}$ (pointing right and down) and $\hat{s}$ (pointing right and up). Only the regions of $\hat{s}$ included in the integration [see Eqs. (73),(74)] have been shaded. The branching ratios are obtained by adding the integrals over the dark- and light-shaded areas, while the asymmetries require subtracting the integral over the light-shaded region from the integral over the dark-shaded region.

As usual, we normalize the branching ratio to the semileptonic decay rate $b\to c\,e\,\bar{\nu}_e$ in order to eliminate the large dependence on the b quark mass: $\Gamma_{\ell\ell}\to\hat{\Gamma}_{\ell\ell}\equiv\Gamma_{\ell\ell}/\Gamma_{b\to c}$, hence

$$\mathrm{BR}_{\ell\ell} = (\mathrm{BR}_{b\to c}) \int d\hat{s}\, 2 \int_0^{\hat{y}_{\max}} d\hat{y} \left(\frac{d^2\hat{\Gamma}_{\ell\ell}}{d\hat{s}\, d\hat{y}} \right)_{\mathrm{symm}}, \quad (75)$$

$$A_{\ell\ell} \equiv \frac{N(y_- > y_+) - N(y_+ > y_-)}{N(y_- > y_+) + N(y_+ > y_-)} = -\frac{1}{\hat{\Gamma}_{\ell\ell}} \int d\hat{s}\, 2 \int_0^{\hat{y}_{\max}} d\hat{y} \left(\frac{d^2\hat{\Gamma}_{\ell\ell}}{d\hat{s}\, d\hat{y}} \right)_{\mathrm{antisymm}} \quad (76)$$

in which the symmetric (antisymmetric) rate must include only the kinematic coefficients symmetric (antisymmetric) in the exchange $\hat{y} \to -\hat{y}$.

We have also calculated some polarization asymmetries, namely the rate when one of the lepton's spin is parallel to its momentum versus the rate when that spin is antiparallel to the momentum. We have considered both the integral of the asymmetry in the differential rates, and the asymmetry in the integrated rates, and also looked at the three possible polarization directions, using the work of Ref. [40].

Let now discuss the impact of the MGM model in the $b \to s\ell^+\ell^-$ decays. The contribution of the MSSM to $C_{9,10}(M_W)$ is given by the γ and Z penguin diagrams proportional to the form factor γ_μ, and by the box diagrams. Their contribution are incorporated into the Y, Z, and E expressions. Inside the penguin and box diagrams can run the charged Higgs bosons, charginos, gluinos, and neutralinos. Since P_E is two orders of magnitude smaller than P_0, and the SUSY contribution to E should be smaller or comparable to the SM one, we will neglect the E contribution in our analysis. The complete analytical results for Y^{SUSY} and Z^{SUSY} can be found in Refs. [12,16].

In the MGM model we have computed the SUSY contribution due to chargino, gluino, and neutralino exchange in the γ and Z penguin diagrams and box diagrams and we find that Y^{SUSY} and Z^{SUSY} are very small comparing to the leading SM contributions, roughly a few percent. (Note that the squarks are quite heavy, but there is no compensating large $\tan\beta$ enhancement.) Also the charged-Higgs-boson contribution to Y and Z is small, being suppressed by at least $\mathcal{O}(m_s/m_b)$ and in practice it is of order of a few percent in both the penguin and box diagrams.

New chirality violating four-fermion operators could be generated at the squark mass with their chiral suppression partially compensated for by $\tan\beta$. However, we found that their contribution is small compared to the leading SM contribution to $C_{9,10}(M_W)$, at least for large squark masses $\mathcal{O}$(0.5–1 TeV).

Thus we find that the only relevant effect of the MGM on the $b \to s\ell^+\ell^-$ decays can be parametrized by R_7 in Eq. (43). In particular for the BR_{ll} and $A_{\ell\ell}$ we find [35]

$$10^7 \times \mathrm{BR}_{ee} = 68.5 + 22.4R_7 + 6.1R_7^2, \quad (77)$$

$$A_{ee} = (4.52 - 3.01R_7)/(10^7\ \mathrm{BR}_{ee}), \quad (78)$$

$$10^7\ \mathrm{BR}_{\mu\mu} = 44.64 + 2.46R_7 + 1.81R_7^2, \quad (79)$$

$$A_{\mu\mu} = (4.68 - 2.90R_7)/(10^7\ \mathrm{BR}_{\mu\mu}), \quad (80)$$

$$10^7\ \mathrm{BR}_{\tau\tau} = 2.013 - 0.201R_7 + 0.009R_7^2, \quad (81)$$

$$A_{\tau\tau} = (0.434 - 0.042R_7)/(10^7\ \mathrm{BR}_{\tau\tau}). \quad (82)$$

The coefficients of these R_7 polynomials were obtained using the same central values for the SM parameters used in the $b \to s\gamma$ decay. We have checked the sensitivity of these predictions to the various input parameters and to the scale μ_b. The main sources of uncertainty are m_t, $\alpha_s(m_Z)$, and the residual μ_b dependence. We find that these uncertainties affect the normalizations of the $\mathrm{BR}_{\ell\ell}$ by up to $\mathcal{O}(10\%)$. However, the uncertainties on the functional dependence on R_7 are much less, at the percent level. There is a small sensitivity to R_8 (which nonetheless can be included). The normalizations of A_{ee} and $A_{\mu\mu}$ are even more sensitive than the branching ratios to μ_b, but an improved SM NLO calculation can reduce the uncertainties to less than $\sim 10\%$. On the contrary the τ forward-backward asymmetry $A_{\tau\tau}$ has a weaker functional dependence on R_7 then the other decay modes. Moreover, we find that the various integrated polarization asymmetries are not particularly sensitive—at most at the few percent level—to R_7, so they would not serve to test this model and we do not include them in our final results.

Finally we would like to stress that when the present residual μ_b dependence is reduced by improving the SM NLO calculation, and when more precise measurements of m_t and $\alpha_s(m_Z)$ are available, then the MGM model predictions for $\mathrm{BR}_{\ell\ell}$ and A_{ll} can be significantly sharpened.

V. $g_\mu - 2$

The anomalous magnetic moment of the muon $a_\mu \equiv (g_\mu - 2)/2$ is one of the most important high precision experiments, providing extremely precise tests of QED and electroweak interactions as well as strong contraints on new physics models. The theoretical prediction is known to $\mathcal{O}(\alpha^5)$ in QED [41], and recently also the two-loop electroweak radiative corrections have been included [42]. The agreement between the theoretical prediction and the experimental result is impressive, but not exact. The current average experimental value of a_μ^{exp} is [43]

$$10^{10} a_\mu^{\mathrm{exp}} - (11\ \ 659\ \ 000) = 230 \pm 84. \quad (83)$$

The E821 experiment at Brookhaven National Laboratory (BNL) is expected to measure a_μ to within $\pm 4 \times 10^{-10}$, or perhaps even $\pm 1 - 2 \times 10^{-10}$ [44]. The most up to date theoretical prediction in the SM is given by the sum of the following contributions [45]:

$$10^{10}a_\mu^{\rm SM}=a_\mu^{\rm QED}+a_\mu^{\rm EW}+a_\mu^{H(1)}(\text{vac pol})+a_\mu^{H(2)}(\text{vac pol}) + a_\mu^{H}(\gamma\times\gamma), \tag{84}$$

where

$$a_\mu^{\rm QED}=11\ \ 658\ \ 470.57\ \ (0.19), \tag{85}$$

$$a_\mu^{\rm EW}=15.1\ \ (0.4), \tag{86}$$

$$a_\mu^{H(1)}(\text{vac pol})=701.1\ \ (9.4), \tag{87}$$

$$a_\mu^{H(2)}(\text{vac pol})=-10.1\ \ (0.6), \tag{88}$$

$$a_\mu^{H}(\gamma\gamma)=-7.92\ \ (1.54). \tag{89}$$

$a_\mu^{\rm QED}$ includes [46] the most recent pure QED contributions at order α^5, $a_\mu^{\rm EW}$ includes the two-loop [42] electroweak corrections, $a_\mu^{H(1,2)}$(vac pol) include, respectively, the one-loop [47] and two-loop [48] hadron vacuum polarization corrections extracted with dispersion relations from the measurement of the $e^+e^-\to$hadrons cross section, and $a_\mu^H(\gamma\gamma)$ contains the hadronic ''light-by-light scattering'' contribution [49].

The hadronic contribution to the vacuum polarization is the largest source of error, reflecting the large experimental uncertainty of the data. However, with the new experiments of BEPC at Beijing, DAΦNE at Frascati, and VEPP-2M at Novosibirsk the theoretical error in a_μ^H(vac pol) will be significantly reduced [50]. The hadronic light-by-light contribution arises from a different class of diagrams which cannot be directly extracted from experimental data, and therefore a somewhat model-dependent calculation is used.

Finally, by combining the results of Eqs. (84)–(89) and summing the errors in quadrature we arrive at the following SM prediction:

$$10^{10}a_\mu^{\rm SM}-(11\ \ 659\ \ 000)=170\pm 10. \tag{90}$$

The improved experimental precision in the next experiment at BNL and the reduction of the theoretical uncertainties in the hadronic vacuum polarization will allow a direct test of the electroweak corrections.

The expected deviations from $a_\mu^{\rm SM}$ induced by the MSSM, and the degree to which the MSSM can be constrained by improved experimental measurements, has been studied since the early days of supersymmetric phenomenology [20]. More recently the impact of large $\tan\beta$ was considered, first in the context of gravity-mediated SUSY breaking [21], next in the general MSSM [22], and finally specifically in gauge-mediated scenarios [23]. However, in this last work, the crucial parameters μ, $\tan\beta$, and the sign of the new amplitudes were not predicted by the model. In contrast, in the MGM model we consider all three of these crucial parameters are predicted along with the rest of the MSSM spectrum in terms of our two fundamental parameters, allowing us to correlate our a_μ prediction with the predictions of $b\to s\gamma$ and $b\to s\ell^+\ell^-$.

The MSSM contributes to a_μ mainly via magnetic-dipole penguin diagrams, with an exchange of a chargino or a neutralino in the loop. We have calculated these contributions and our analytical results are in agreement, in magnitude and sign, with the results of Ref. [22] (after accounting for the erratum).

In the MGM model the chargino amplitudes dominate the neutralino ones, and within the chargino contribution the terms proportional to the chargino mass completely dominate. Using also $v_D \ll v_U$ yields [35], for the deviation from the standard model,

$$\Delta a_\mu^{\rm MGM}\simeq a_\mu^{\tilde h^-}\simeq\frac{3\alpha_2}{4\pi}\tan\beta\frac{m_\mu^2\mu M_2 F_\mu(x_{\tilde h_1\tilde\nu},x_{\tilde h_2\tilde\nu})}{m_{\tilde\nu}^2(M_{\tilde h_1^-}^2-M_{\tilde h_2^-}^2)}, \tag{91}$$

where

$$F_\mu(x_1,x_2)=f_\mu(x_1)-f_\mu(x_2), \tag{92}$$

$$f_\mu(x)=\frac{3-4x+x^2+2\ln x}{3(1-x)^3},$$

and $x_{\tilde h_i\tilde\nu}=M_{\tilde h_i^-}^2/m_{\tilde\nu}^2$. For our numerical results we will use the complete expressions for $a_\mu^{\rm MGM}$.

VI. MGM MODEL PREDICTIONS

As explained in Sec. II, when the self-consistent equation Eq. (24) for $\tan\beta$ is numerically solved, all of the relevant SUSY spectrum and physical quantities can be predicted as a function of only two fundamental parameters: the effective SUSY-breaking scale Λ or equivalently the weak gaugino mass M_2, and the logarithm of the common messenger mass M_M. In principle these results will depend on the doublet and triplet messenger mass splitting, but the dependence is very weak for the expected small splitting. In all our computations we will assume that $M_{M_3}=1.3M_{M_2}$.

We consider the range $2\Lambda<M_M<10^4\Lambda$. Messenger masses much nearer to the absolute lower bound Λ (below which their scalar components would develop VEVs) are not of much interest: they are either already ruled out by vacuum stability constraints [11] or require extremely heavy superpartners and thus mimic the standard model. Messenger masses much above $\mathcal{O}(10^4\Lambda)$ may also destabilize the

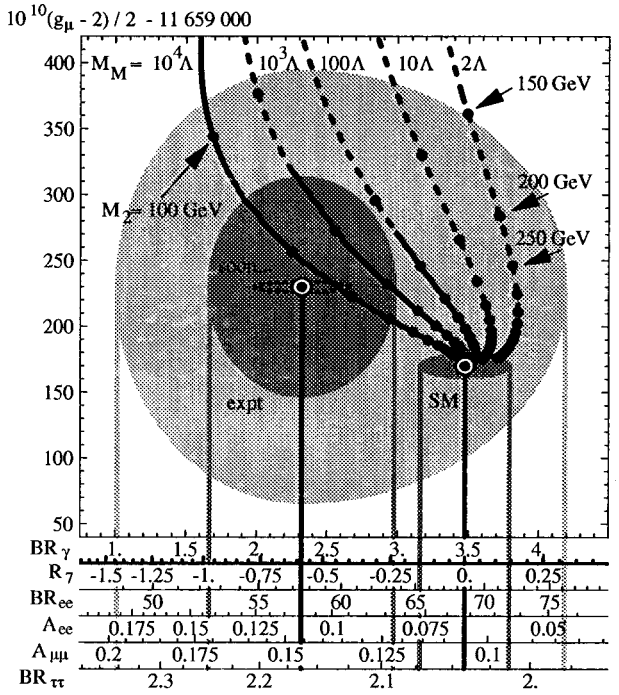

FIG. 2. The $N=1$ MGM predictions of BR_γ ($\times 10^4$) and $10^{10}(g_\mu - 2) - 1165900$ as functions of the W-ino mass M_2, for various messenger masses M_M and with heavy dots at discrete M_2 values. The experimental and SM central values, indicated with circled dots, are surrounded by the corresponding uncertainty ellipses. The extra horizontal axes are the correlated predictions for R_7, $\mathrm{BR}_{\ell\ell}$ ($\times 10^7$), and $A_{\ell\ell}$.

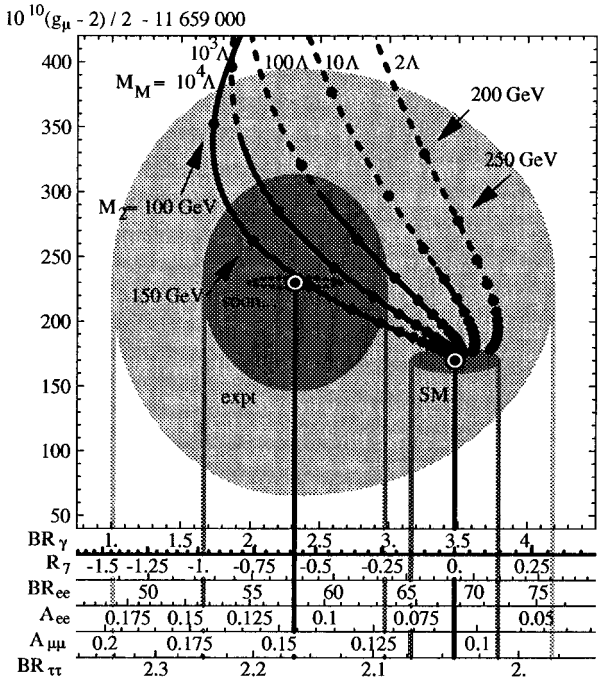

FIG. 3. The MGM predictions as in Fig. 2 but for $N=2$.

vacuum or run into cosmological difficulties with a heavy gravitino (see Refs. [11,51], and references therein), though this is by no means an airtight bound.

Within this range of M_M, the one-step solution we have used for the RG equations is an adequate approximation. In the low M_M region, $\tan\beta$ is ~ 50 and there are strong cancellations in the B term and in the $b \to s\gamma$ amplitudes, so an accurate solution is required. But as shown in Ref. [11], the one-step approximation in this case is as accurate as keeping only the leading threshold corrections, and both of these approximations are entirely sufficient for our purposes. For the highest values of M_M we consider, the one-step approximation is not as accurate, but the cancellations in B and in $b \to s\gamma$ are not as severe, so the reduced accuracy is once again sufficient. In the end, we estimate that the uncertainties in our predictions of BR_γ and a_μ are comparable to the corresponding SM ones.

In Figs. 2 and 3 we present our MGM model predictions as a function of M_M and the weak gaugino mass M_2 for $N=1$ or 2 messenger families, respectively. Different curves are given for different messenger masses M_M, and heavy dots indicate discrete values of M_2. The SM-predicted and measured central values are shown as circled dots. The dark and light gray areas surrounding the experimental central value indicate the regions allowed at $1\,\sigma$ and 95% C.L., respectively. The dark ellipse surrounding the central value of the SM predictions indicates the expected theoretical uncertainty, which should also be applied to each point on the MGM prediction curves. Finally, the small dashed ellipse centered (for the present) on the experimental central value indicates the $1\,\sigma$ uncertainties expected in the near future from BNL and CLEO.

The heavy (continuous and dashed) curves are our predictions for a_μ along the vertical axis, and either BR_γ or any of the various $B \to X_s l^+ l^-$ branching ratios and asymmetries. All the latter are correlated in their dependence on the single parameter R_7 which measures the deviation from the SM of the amplitude of the Q_7 operator. At present BR_γ is by far the best measure of R_7, which is why we emphasize it in our graphs. (The various quantities along the horizontal axes depend slightly and differently on the R_8 parameter, so to present them in the same graph we have chosen a specific value of $R_8 = 0$. But we estimate that this approximation affects the R_7 predictions by an uncertainty that is well within the SM one shown in the figure.) The curves become dashed for those ranges of M_M and M_2 which are in fact ruled out by vacuum stability constraints [11], primarily due to the stau developing a charge-breaking VEV.

Several features of the MGM model predictions stand out from these figures.

(1) When the messengers are relatively heavy, the MGM predictions are in better agreement with experiment than those of the SM (except for extremely light superpartners): when the superpartners are lowered (to their natural values, around the electroweak scale) and the MGM departs from the SM, a_μ increases and BR_γ decreases towards the experimental central value. In particular, the sign of this effect is a prediction of the MGM.

(2) When the messengers are quite light, a fortuitous cancellation between the chargino and charged-Higgs ampli-

tudes in R_7 prevents BR_γ and the various $B\to X_s l^+ l^-$ branching ratios and asymmetries from deviating significantly from the SM, although a_μ is still raised as before.

(3) The expected reduction in experimental uncertainty will tremendously sharpen the comparison with the SM and MGM predictions, possibly deciding between the two and definitely strongly constraining the latter.

(4) At present, the (absolute) bounds vaccum instability bounds on M_M and M_2 are stronger than the (95% CL) experimental bounds due to BR_γ and a_μ.

As a function of N the sfermion masses scale as $1/\sqrt{N}$ relative to the gauginos [see Eqs. (3)–(8)]. Raising N for fixed gaugino masses thus lowers the sfermions and amplifies the MGM effects. While this is the general trend, in practice there are some complications because of cancellations and the variation in $\tan\beta$. By comparing Figs. 2,3 throughout the allowed region for fixed values of M_M and M_2, we see that when N is increased, R_7 (or equivalently BR_γ) is decreased and a_μ is increased. Raising N is roughly equivalent to lowering M_2 while raising M_M.

From the horizontal axes below those of BR_γ and R_7 in Figs. 2,3, our predictions for BR_{ee}, $\mathrm{BR}_{\tau\tau}$, A_{ee}, and $A_{\mu\mu}$ may be read off. We do not give the results for $\mathrm{BR}_{\mu\mu}$ and $A_{\tau\tau}$ because they are not very sensitive to R_7. Evidently the MGM model can produce large deviations from the SM in A_{ee} and $A_{\mu\mu}$, and somewhat smaller ones in BR_{ee} and $\mathrm{BR}_{\mu\mu}$. Note however that the $b\to s\ell^+\ell^-$ quantities have their own theoretical uncertainties beyond those indicated in the figures, mainly from the residual μ_b dependence, as explained in Sec. IV. These could be reduced by improving the SM NLO (in α_s) calculations, at which point the MGM model would predict the branching ratios and asymmetries more precisely. We expect that at least some of these predictions could be tested at hadronic colliders in the next few years.

VII. CONCLUSIONS

Within the minimal gauge-mediated SUSY-breaking model, which can naturally generate a large $\tan\beta$, we have computed the inclusive branching ratio $B\to X_s\gamma$, the inclusive branching ratios and asymmetries for $B\to X_s\ell^+\ell^-$ (with $\ell=e,\mu,\tau$), and the anomalous magnetic moment of the muon $a_\mu\equiv(g_\mu-2)/2$. In particular we included the complete next-to-leading order accuracy in the strong coupling for the B decays.

The MGM model, described in Sec. II, has a naturally high $\tan\beta$ signature provided that the tree-level soft-breaking B parameter, which couples the Higgs doublets in the scalar potential, vanishes. Moreover this model is highly predictive: all the SUSY soft-breaking terms, as well as $\tan\beta$ and the physical relative sign (often called the sign of the μ parameter), can be predicted in terms of only two fundamental parameters: the SUSY breaking scale (or equivalently the W-ino mass), and the logarithm of a common messenger mass. Therefore the MGM predictions for these processes are strongly correlated.

The correlated predictions are shown in Figs. 2 and 3. Note that the correlation between a_μ and BR_γ depends on the model parameters M_M or M_2 whereas the various b-quark-related quantities are all completely correlated through their dependence on the single quantity R_7 independent of M_2 and M_M (a quite general feature of the MSSM, as discussed in Ref. [18]). We have gone slightly beyond the minimal model by including the results for $N=2$ messenger families. We included the results of the numerical predictions for $N=1$ and $N=2$ messenger families in Figs. 2 and 3, respectively. The general trend of the MGM predictions emerging from these results can be summarized as follows:

When the messenger scale is a few orders of magnitude above $\Lambda\sim\mathcal{O}(100\,\mathrm{TeV})$, and the superpartners are near their natural electroweak scale, the MGM predicts a higher anomalous magnetic moment and lower $b\to s\gamma$ branching ratio than the SM, in agreement with present measurements.

When the messengers are not far above Λ, the superpartners must be significantly higher than the electroweak scale, and (due to a cancellation) the $b\to s\gamma$ rate is largely unperturbed from its SM value, though the anomalous magnetic moment is raised.

Increasing the number of messenger families amplifies these predictions somewhat: it is similar to lowering the superpartner scale and raising the messenger scale.

At present, the allowed range of M_2 and M_M values is more constrained by theoretical vacuum-stability constraints than by experimental data on BR_γ and a_μ, though that data does mildly favor the MGM model over the standard one. However, the BNL a_μ experiment now in progress, and the much-awaited CLEO analysis of their BR_γ measurements, will dramatically constrain the MGM and allow a much more convincing discrimination between the two models. Measurements of several $B\to X_s\ell^+\ell^-$ branching ratios and asymmetries at hadron colliders should further sharpen the b-quark side of this picture in the next few years.

Note added. After this work was completed, new and significant theoretical results on radiative b decay have appeared, one [52] taking into account the proper electroweak radiative corrections and the other [53] convincingly criticizing the current method of extracting the inclusive rate for $b\to s\gamma$ from the currently published CLEO data. The former slightly lowers the SM prediction, while the latter argues that theoretical uncertainties have so far been underestimated, and that only with more new data on the spectrum or with an improved m_b value from upsilon spectroscopy can the uncertainties be reduced. Thus, though at present it is difficult to sharply compare the predicted inclusive decay rate with experiment, we expect that in the very near future such a comparison will be possible.

ACKNOWLEDGMENTS

We gratefully acknowledge discussions with I. Bigi, A.L. Kagan, T. Moroi, M. Neubert, and C. Wagner. One of us (E.G.) would also like to thank the Physics Department of the University of Notre Dame, where most of this work was done, for its warm and kind hospitality.

[1] F. Gabbiani and A. Masiero, Nucl. Phys. **B322**, 235 (1989); J. S Hagelin, S. Kelley, and T. Tanaka, *ibid.* **B415**, 293 (1994); F. Gabbiani, E. Gabrielli, A. Masiero, and L. Silvestrini, *ibid.* **B477**, 321 (1996).
[2] P. Fayet and S. Ferrara, Phys. Rep., Phys. Lett. **32C**, 249 (1977); H. P. Nilles, *ibid.* **110C**, 1 (1984).
[3] R. Barbieri, L. Hall, and A. Strumia, Nucl. Phys. **B445**, 219 (1995); **B449**, 437 (1995); R. Barbieri, A. Strumia, and A. Romanino, Phys. Lett. B **369**, 283 (1996).
[4] L. Ibanez and D. Lüst, Nucl. Phys. **B382**, 305 (1992); V. Kaplunovsky and J. Louis, Phys. Lett. B **306**, 269 (1993).
[5] M. Dine and A. Nelson, Phys. Rev. D **48**, 1277 (1993); M. Dine, A. Nelson, and Y. Shirman, *ibid.* **51**, 1362 (1995); M. Dine, A. Nelson, Y. Nir, and Y. Shirman, *ibid.* **53**, 2658 (1996).
[6] K.S. Babu, C. Kolda, and F. Wilczek, Phys. Rev. Lett. **77**, 3070 (1996).
[7] M. Dine, Y. Nir, and Y. Shirman, Phys. Rev. D **55**, 1501 (1997).
[8] S. P. Martin, Phys. Rev. D **55**, 3177 (1997).
[9] For a recent review on the gauge-mediated models, see G.F. Giudice and R. Rattazzi, hep-ph/9801271, and reference therein.
[10] G. Dvali, G.F. Giudice, and A. Pomarol, Nucl. Phys. **B478**, 31 (1996).
[11] R. Rattazzi and U. Sarid, Nucl. Phys. **B501**, 297 (1997).
[12] S. Bertolini, F. Borzumati, A. Masiero, and G. Ridolfi, Nucl. Phys. **B353**, 591 (1991).
[13] R. Garisto and J.N. Ng, Phys. Lett. B **315**, 372 (1993); L.J. Hall, R. Rattazzi, and U. Sarid, Phys. Rev. D **50**, 7048 (1994); M.A. Diaz, Phys. Lett. B **322**, 207 (1994); F.M. Borzumati, Z. Phys. C **63**, 291 (1994).
[14] T. Blazek and S. Raby, hep-ph/9712257.
[15] R. Rattazzi and U. Sarid, Phys. Rev. D **53**, 1553 (1996); N.G. Deshpande, B. Dutta, and S. Oh, *ibid.* **56**, 519 (1997); S. Dimopoulos, S. Thomas, and J.D. Wells, Nucl. Phys. **B488**, 39 (1997); F.M. Borzumati, hep-ph/9702307.
[16] P. Cho, M. Misiak, and D. Wyler, Phys. Rev. D **54**, 3329 (1996).
[17] T. Goto, Y. Okada, Y. Shimizu, and M. Tanaka, Phys. Rev. D **55**, 4273 (1997).
[18] J.L. Hewett and J.D. Wells, Phys. Rev. D **55**, 5549 (1997).
[19] J.L. Hewett, Phys. Rev. D **53**, 4964 (1996).
[20] J.A. Grifols and A. Mendez, Phys. Rev. D **26**, 1809 (1982); J. Ellis, J.S. Hagelin, and D.V. Nanopoulos, Phys. Lett. **116B**, 283 (1982); R. Barbieri and L. Maiani, *ibid.* **117B**, 203 (1982); D.A. Kosower, L.M. Krauss, and N. Sakai, *ibid.* **133B**, 305 (1983); T.C. Yuan, R. Arnowitt, A.H. Chamseddine, and P. Nath, Z. Phys. C **26**, 407 (1984); J.C. Romao, A. Barroso, M.C. Bento, and G.C. Branco, Nucl. Phys. **B250**, 295 (1985); J.L. Lopez, D.V. Nanopoulos, and X. Wang, Phys. Rev. D **49**, 366 (1994); H. Konig, Mod. Phys. Lett. A **10**, 1113 (1995).
[21] U. Chattopadhyay and P. Nath, Phys. Rev. D **53**, 1648 (1996).
[22] T. Moroi, Phys. Rev. D **53**, 6565 (1996); **56**, 4424(E) (1997).
[23] M. Carena, G.F. Giudice, and C.E.M. Wagner, Phys. Lett. B **390**, 234 (1997).
[24] K. Chetyrkin, M. Misiak, and M. Munz, Phys. Lett. B **400**, 206 (1997).
[25] M. Misiak, Nucl. Phys. **B393**, 23 (1993); **B439**, 461(E) (1995).
[26] A.J. Buras and M. Munz, Phys. Rev. D **52**, 186 (1995).
[27] G.F. Giudice and R. Rattazzi, Nucl. Phys. **B511**, 25 (1998).
[28] Y. Grossman, Y. Nir, and R. Rattazzi, in ''Heavy Flavours II,'' edited by A. J. Buras and M. Lindner, Advanced Series on Directions in High Energy Physics (World Scientific, Singapore, in press), hep-ph/9701231.
[29] CLEO Collaboration, M.S. Alam *et al.*, Phys. Rev. Lett. **74**, 2885 (1995).
[30] A.F. Falk, M. Luke, and M. Savage, Phys. Rev. D **49**, 3367 (1994).
[31] M.B. Voloshin, Phys. Lett. B **397**, 275 (1997); A. Khodjamirian, R. Ruckl, G. Stoll, and D. Wyler, *ibid.* **402**, 167 (1997); Z. Ligeti, L. Randall and M.B. Wise, *ibid.* **402**, 178 (1997); A.K. Grant, A.G. Morgan, S. Nussinov, and R.D. Peccei, Phys. Rev. D **56**, 3151 (1997).
[32] G. Buchalla, G. Isidori, and S.J. Rey, Nucl. Phys. **B511**, 594 (1998); G. Buchalla and G. Isidori, *ibid.* **B525**, 333 (1998).
[33] A.J. Buras, A. Kwiatkowski, and N. Pott, Phys. Lett. B **414**, 157 (1997).
[34] Particle Data Group, R.M. Barnett *et al.*, Phys. Rev. D **54**, 1 (1996).
[35] E. Gabrielli and U. Sarid, Phys. Rev. Lett. **79**, 4752 (1997).
[36] A. Ali, G.F. Giudice, and T. Mannel, Z. Phys. C **67**, 417 (1995).
[37] A. Ali, G. Hiller, L.T. Handoko, and T. Morozumi, Phys. Rev. D **55**, 4105 (1997); A. Ali, Nucl. Phys. B (Proc. Suppl.) **59**, 86 (1997), and reference therein.
[38] UA1 Collaboration, C. Albajar *et al.*, Phys. Lett. B **262**, 163 (1991); CDF Collaboration, F. Abe *et al.*, Phys. Rev. Lett. **76**, 4675 (1996); D0 Collaboration, S. Abachi *et al.* in *ICHEP'96*, Proceedings of the International Conference on High Energy Physics, Warsaw, Poland, 1996, edited by Z. Ajduk and A. Wroblewski (World Scientific, Singapore, 1997); R. Balest *et al.*, CLEO Collaboration, Report No. CLEO CONF 97-15; D0 Collaboration, B. Abbott *et al.* Phys. Lett. B **423**, 419 (1998).
[39] T. Liu and S. Pakvasa, Report No. UH-511-867-97.
[40] F. Krüger and L. M. Sehgal, Phys. Lett. B **380**, 199 (1996).
[41] T. Kinoshita and W.J. Marciano, in *Quantum Electrodynamics*, edited by T. Kinoshita (World Scientific, Singapore, 1990), p. 419, and references therein.
[42] T.V. Kukhto, E.A. Kuraev, A. Schiller, and Z.K. Silagadze, Nucl. Phys. **B371**, 567 (1992); A. Czarnecki, B. Krause, and W.J. Marciano, Phys. Rev. D **52**, 2619 (1995); Phys. Rev. Lett. **76**, 3267 (1996); S. Peris, M. Perrottet, and E. de Rafael, Phys. Lett. B **355**, 523 (1995).
[43] Particle Data Group, L. Montanet *et al.*, Phys. Rev. D **50**, 1173 (1994).
[44] B.L. Roberts *et al.*, in *ICHEP 96*, [38].
[45] M. Hayakawa and T. Kinoshita, Phys. Rev. D **57**, 465 (1998), and reference therein.
[46] T. Kinoshita, Rep. Prog. Phys. **59**, 1459 (1996).
[47] R. Alemany, M. Davier, and A. Hocker, Eur. Phys. J. C **2**, 123 (1998); CLEO Collaboration, Report No. CLEO CONF 97-31, EPS97 368.
[48] B. Krause, Phys. Lett. B **390**, 392 (1997).
[49] M. Hayakawa, T. Kinoshita, and A.I. Sanda, Phys. Rev. Lett. **75**, 790 (1995); Phys. Rev. D **54**, 3137 (1996); J. Bijnens, E. Pallante, and J. Prades, Phys. Rev. Lett. **75**, 1447 (1995); **75**, 3781(E) (1995); Nucl. Phys. **B474**, 379 (1996).
[50] D.H. Brown and W.A. Worstell, Phys. Rev. D **54**, 3237 (1996); R. Barbieri and E. Remiddi, in *Second DAΦNE Phys-*

ics Handbook, edited by L. Maiani, L. Pancheri and N. Paver (INFN, Franzini, 1995), Vol. II, p. 467; P. Franzini, *ibid.*, p. 471.

[51] S. Ambrosanio, G.L Kane, G.D. Kribs, S.P. Martin, and S. Mrenna, Phys. Rev. D **54**, 5395 (1996); J.A. Bagger, K.T. Matchev, D.M. Pierce, and R. Zhang, *ibid.* **55**, 3188 (1997).

[52] A. Czarnecki and W.J. Marciano, Phys. Rev. Lett. **81**, 277 (1998).

[53] A.L. Kagan and M. Neubert, hep-ph/9805303; and (private communication).